

Article

# Functional Similarity and Difference among *Bra-MIR319* Family in Plant Development

Ziwei Hu <sup>1,2</sup>, Tingting Liu <sup>1,2</sup>  and Jiashu Cao <sup>1,2,3,\*</sup>

<sup>1</sup> Laboratory of Cell and Molecular Biology, Institute of Vegetable Science, Zhejiang University, Hangzhou 310058, China; 11416051@zju.edu.cn (Z.H.); 11416009@zju.edu.cn (T.L.)

<sup>2</sup> Key Laboratory of Horticultural Plant Growth, Development and Quality Improvement, Ministry of Agriculture, Hangzhou 310058, China

<sup>3</sup> Zhejiang Provincial Key Laboratory of Horticultural Plant Integrative Biology, Hangzhou 310058, China

\* Correspondence: jshcao@zju.edu.cn; Tel.: +86-571-8898-2597

Received: 29 October 2019; Accepted: 13 November 2019; Published: 21 November 2019



**Abstract:** miR319 was the first plant miRNA discovered via forward genetic mutation screening. In this study, we found that miR319 family members had similar sequences but different expression patterns in *Brassica campestris* and *Arabidopsis thaliana*. RT-PCR analysis revealed that *Bra-MIR319a* and *Bra-MIR319c* had similar expression patterns and were widely expressed in plant development, whereas *Bra-MIR319b* could only be detected in stems. The overexpression of each *Bra-MIR319* family member in *Arabidopsis* could inhibit cell division and function in leaf and petal morphogenesis. *Bra-miR319a* formed a new regulatory relationship after whole genome triplication, and *Bra-MIR319a* overexpressing in *Arabidopsis* led to the degradation of pollen content and affected the formation of intine, thereby causing pollen abortion. Our results suggest that *Bra-MIR319* family members have functional similarity and difference in plant development.

**Keywords:** *Brassica campestris*; Bra-miR319 family; leaf and petal morphogenesis; pollen development

## 1. Introduction

MicroRNAs (miRNAs) are a class of short (about 21 nt in length) noncoding RNAs [1]. In plants, different miRNA precursor genes can form the same or similar mature sequences, and these precursor genes are considered to be the same family [2,3]. miRNA family members have similar functions due to the same or similar mature sequences. However, each precursor gene in the miRNA family has different expression patterns and targets, so they exhibit functional differentiation [4].

miR319 was the first plant miRNA discovered via forward genetic mutation screening; leaves of the mutant *jaw-D* are crinkly and serrated [5]. In *Arabidopsis thaliana*, three precursor genes of miR319 can produce two mature sequences, which differ by one base at the 3' end [6]. The three members of *MIR319* have different expression patterns. *MIR319a* is continuously expressed during plant growth, *MIR319b* is expressed only during vegetative growth, and *MIR319c* is highly expressed in reproductive growth [7]. Different expression patterns lead to differences in gene function. The overexpression of *MIR319a* results in leaf phenotypes similar to those of *jaw-D* mutants, whereas leaves of overexpressing *MIR319c* plants have no difference with those of wild-type plants [6]. The expression level of miR319a is higher than those of miR319b and miR319c. Thus, the current report on the regulation of the miR319 family mainly focuses on miR319a. miR319a can target five TCP transcription factors but also some MYB transcription factors in *A. thaliana* [6,7]. miR319a participates in leaf morphogenesis by targeting *TCPs* [8,9]. Given the cross-target of miR319 and miR159, the overexpression of *MIR319a* causes anther defects similar to those seen in overexpressing *MIR159a* plants [6]. High-throughput

sequencing has revealed that miR319 is also present in pollen [10], but its role in pollen development is unclear.

*Brassica campestris* (syn. *B. rapa*) and *A. thaliana* are closely related in taxonomy [11]. Compared with *A. thaliana*, *B. campestris* undergoes whole-genome triplication (WGT), its genome is divided into three subgenomes, and the number and expressions of genes are differentiated in three subgenomes [12]. Similar to the encoded protein gene family, miRNA families also undergo functional retention and differentiation in *B. campestris* after WGT [13,14]. Moreover, the complexity of miRNAs regulating target genes is increased after gene duplication. miRNA target genes undergo a high degree of differentiation, and some miRNA binding sites are lost [15,16].

We previously used the precursor gene of miR319 in *A. thaliana* to perform BLAST in the Brassica database (<http://brassicadb.org/brad/>) and obtained the precursor genes of Bra-miR319 [17]. The similarity of miR319 precursor sequences between *B. campestris* and *A. thaliana* was over 80%. Bra-miR319a and Bra-miR319b had the same sequence, whereas Bra-miR319c had one base difference at the 3' end. They shared the same sequences with those of *A. thaliana*. In this study, we found that although their sequences were highly conserved in *B. campestris* and *A. thaliana*, Bra-miR319 family members had different expression patterns than those in *A. thaliana*, and they could all function in leaf and petal morphogenesis. Moreover, Bra-miR319a could also target *BcMYB101* and function in pollen development. Our results indicate that after WGT, *Bra-MIR319* family members had functional similarity and difference in plant development.

## 2. Materials and Methods

### 2.1. Plant Materials

Chinese cabbage “Aijiaohuang” (*B. campestris* L. subsp. *chinensis* Makino cv. Aijiaohuang) was cultivated in the experimental farm of Zhejiang University. *A. thaliana* (Col-0), transgenic plants, and nuclear localization tobacco (*Nicotiana benthamiana*) were grown under long-day conditions (16 h light/8 h dark) at 22 °C.

### 2.2. Expression Profile Analysis

The total RNA and small RNA from roots, stems, leaves, inflorescences, and siliques were extracted by using a microRNA extraction kit (Invitrogen, Carlsbad, CA, USA) and reversed transcribed into the first strand of cDNA through the PrimerScript RT reagent kit (TAKARA, Shiga, Japan). *BcUBC10* and *BcU6* were selected as the reference genes for RT-PCR and qRT-PCR; the gene-specific primers are listed in Supplementary Materials Table S1. qRT-PCR was performed by using the SYBR<sup>®</sup> Premix Ex Taq<sup>™</sup> Kit (TaKaRa, Shiga, Japan) in a CFX96 Real-Time System (Bio-Rad, Hercules, CA, USA). The  $2^{-\Delta\Delta Ct}$  method was used to compute the expression levels of different genes [18].

### 2.3. Generation of Bra-MIR319-Overexpression Arabidopsis Lines

The 168 bp precursor gene of *Bra-MIR319a*, 169 bp precursor gene of *Bra-MIR319b*, and 161 bp precursor gene of *Bra-MIR319c* were amplified with gene-specific primer pairs (Supplementary Table S1) and subcloned into the pBI121 vector with the constitutive *CaMV 35S* promoter, respectively. These constructs were transferred into the *Arabidopsis* plant through the floral-dip method mediated by *Agrobacterium* [19]. The seeds of transformed *Arabidopsis* were screened in 1/2 MS agar plate containing kanamycin. The total RNA from the transgenic plants and wild-type plants were extracted and the expression levels of *Bra-MIR319a*, *Bra-MIR319b*, and *Bra-MIR319c* were detected via qRT-PCR in accordance with the abovementioned method. Transgenic T<sub>1</sub> plants were used for the phenotypic observation of vegetative growth and T<sub>2</sub> plants were further used for the observation of pollen development.

#### 2.4. Morphological and Cytological Observation

The methods for scanning electron microscopy (SEM) and transmission electron microscopy (TEM) observation were previously described [20]. Semithin section observations of leaf and anther were previously described [21]. Image-Pro software was used to measure the size of epidermal cells at 1 K magnification. Alexander staining was used to observe pollen vitality.

#### 2.5. Cleavage Site of miRNA Targets

The miRNA target gene prediction website (<http://plantgrn.noble.org/psRNATarget/>) was used to predict the target genes of Bra-miR319. Total RNA was purified to extract poly (A) RNA. cDNA was synthesized using the RACE kit (TAKARA). Nested PCR was performed for 5' rapid amplification of cDNA ends (RACE) with specific reverse primers (Supplementary Table S1).

#### 2.6. Transient Expression in *N. benthamiana*

The CDS of *BcMYB101* was cloned into pFGC-eGFP to create the fusion construct by using gene-specific primer pairs (Supplementary Table S1). As a control, we amplified the CDS of *mBcMYB101* with multiple mutations in the miRNA complement motif, preventing the miRNA from cleaving without altering its amino acid sequence, and cloned it into pFGC-eGFP via overlapping PCR. The method of coexpression of Bra-miR319a and *BcMYB101* was described previously [6]. After 48 h of transfection, GFP fluorescence was detected using a confocal laser scanning microscope (Nikon A1-SHS, Japan).

### 3. Results

#### 3.1. Bra-MIR319 Family Members Have Functional Similarity in Leaf and Petal Morphogenesis

Expression of Bra-miR319 was detected via qRT-PCR in different tissues of *B. campestris*, including roots, stems, leaves, inflorescences, and siliques. The result showed that Bra-miR319 was expressed in all tissues, and its expression in the stem was higher (Figure 1a). Given that Bra-miR319 could be produced by different precursors, the expression of these precursors was detected via RT-PCR. The expressions of *Bra-MIR319a* and *Bra-MIR319c* were similar, and *Bra-MIR319b* was only expressed in stems (Figure 1b). We constructed overexpression vectors for *Bra-MIR319a*, *Bra-MIR319b*, and *Bra-MIR319c*, respectively, and transferred them into the *Arabidopsis* plants to observe the phenotype of transgenic plants. Expressions of *Bra-MIR319a*, *Bra-MIR319b*, and *Bra-MIR319c* were all increased in transgenic *Arabidopsis* plants (Figure S1). p35S: *Bra-MIR319a*, p35S: *Bra-MIR319b*, and p35S: *Bra-MIR319c* transgenic *Arabidopsis* plants could all show crinkly leaves (Figure 2b–d). Further, transgenic *Arabidopsis* plants also showed wavy and yellow-green petals (Figure 2e–h). Compared with the wild-type petal, the petal vascular tissue of the transgenic plants exhibited an irregular shape (Figure 2i–l). These results indicated that all precursor genes of Bra-miR319 could be efficiently processed in *Arabidopsis*, and they had similar functions in leaf and petal morphogenesis.

#### 3.2. Bra-MIR319 Family Members Overexpressing in *Arabidopsis* Can Inhibit Cell Division

We selected the fifth leaf of the fully expanded transgenic and wild-type *Arabidopsis* plants for further cytological observation. SEM showed that the overexpression of *Bra-MIR319a*, *Bra-MIR319b*, and *Bra-MIR319c* reduced the number of epidermal cells in *Arabidopsis* leaves, but the cells increased in size (Figure 3a–d,i). The size of the epidermal cells of wild-type and transgenic plants were measured by Image-Pro software at 1 K magnification. The size of the epidermal cells of the wild-type plants was  $1258.8 \pm 545.8 \mu\text{m}^2$ , and the size of the epidermal cells of *Bra-MIR319* family members overexpressing plants was  $1835.1 \pm 666.1$ ,  $2612.5 \pm 152.6$ , and  $1687.2 \pm 518.2 \mu\text{m}^2$ , respectively. Comparing the shape of leaf epidermal cells, it was found that cells of the wild-type plants were "jigsaw", while the epidermal cells of the transgenic plants were rounder and showed undifferentiated cell morphology. The results of semithin section analysis showed that the number and arrangement of palisade tissues in leaves

of transgenic plants were not different from those of wild-type plants, but the number of sponge tissues was significantly less than that of wild-type plants (Figure 3e–h,j–k). These results indicated *Bra-MIR319a*, *Bra-MIR319b*, and *Bra-MIR319c* were involved in cell division and differentiation.

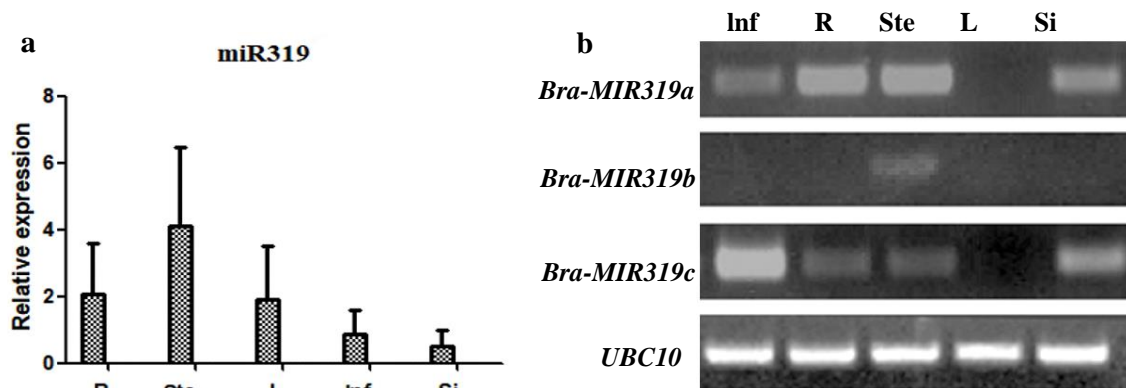


**Figure 1.** Expression pattern of Bra-miR319 family members. (a) Quantitative real-time PCR analysis of Bra-miR319 in different tissues of *Brassica campestris*. (b) Real-time PCR analysis of precursor genes of Bra-miR319 in different tissues of *B. campestris*. Roots (R), stems (Ste), leaves (L), inflorescences (Inf), and siliques (Si).

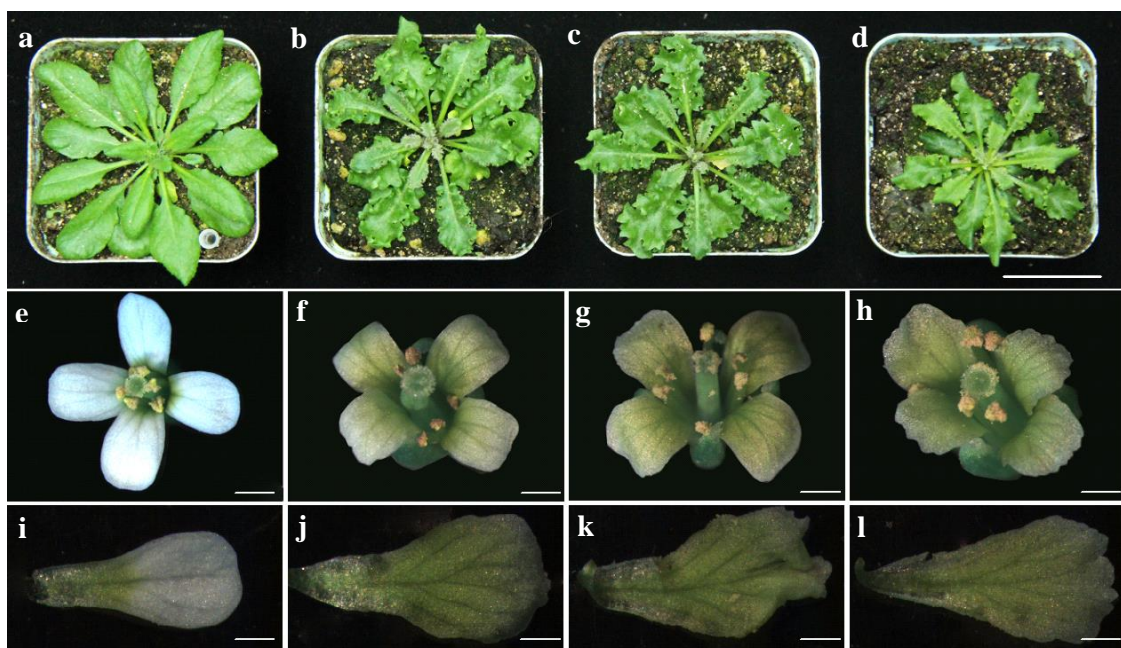


**Figure 2.** Phenotype of *Bra-MIR319* family overexpressing transgenic *Arabidopsis*. (a–d) Rosette plants of wild-type and overexpressing the *Bra-MIR319a*, *Bra-MIR319b*, and *Bra-MIR319c*, respectively. (e–h) The flower of wild-type plant and transgenic *Arabidopsis* overexpressing the *Bra-MIR319* family, respectively. (i–l) The petal of wild-type plant and transgenic *Arabidopsis* overexpressing the *Bra-MIR319* family, respectively. Scale bars, 2 mm in (a–d), 1 mm in (e–l).

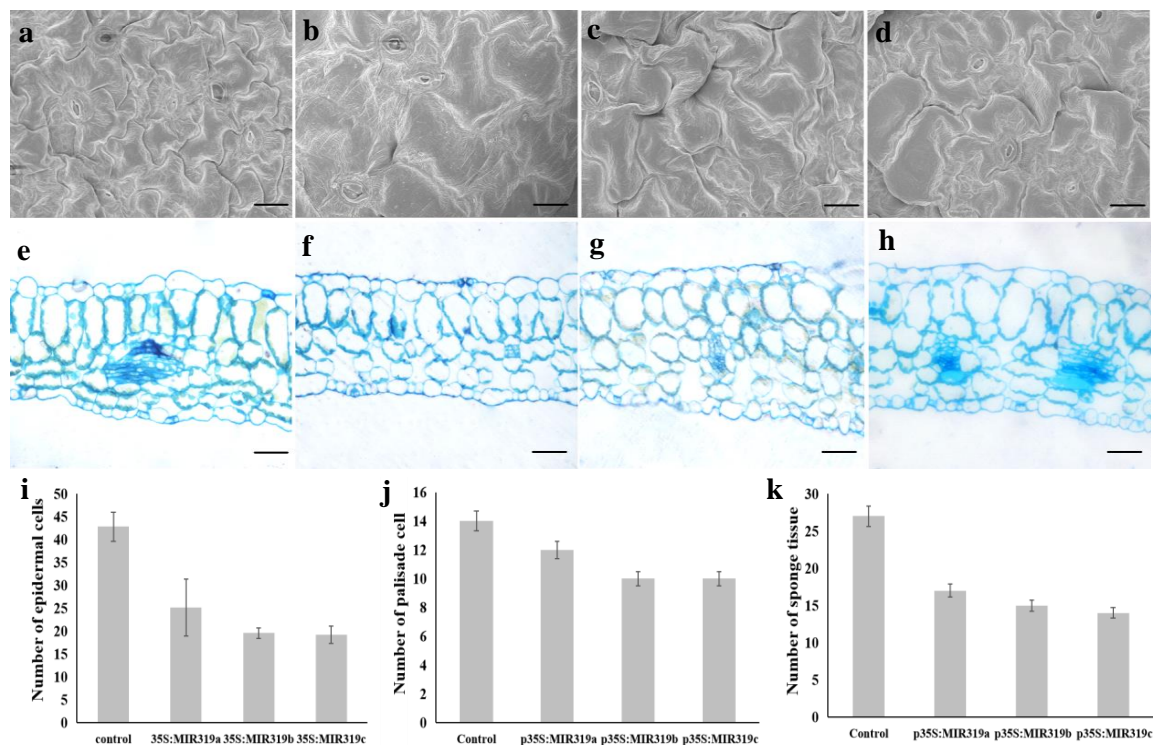


**Figure 3.** SEM and semithin section observation of leaf cells in transgenic *Arabidopsis* overexpressing the *Bra-MIR319* gene family. (a–d) SEM observation of leaf epidermal cell of wild-type plants and *Bra-MIR319* family transgenic *Arabidopsis*, respectively. (e–h) Observation of leaf structure of wild-type plants and *Bra-MIR319* family transgenic *Arabidopsis*, respectively, via semithin section analysis. (i–k) Statistical analysis of leaf epidermal cells, palisade tissue, and sponge tissue cells under 1 K magnification. Scale bars, 50  $\mu$ m.

### 3.3. *Bra-MIR319a* Overexpressing in *Arabidopsis* Reduces Pollen Viability

We further observed the reproductive growth of transgenic plants. We examined the pollen viability and morphology of *Bra-MIR319a*, *Bra-MIR319b*, and *Bra-MIR319c* overexpressing plants. Alexander staining results showed that nearly 86.4% of the pollen in the p35S:*Bra-MIR319a* anthers was blue-green, and only a small part of the pollen was viable. In contrast, the pollen stainings of *Bra-MIR319b* and *Bra-MIR319c* transgenic plants were indistinguishable from those of wild-type plants, and both pollen grains were viable (Figure 4a–d). The pollen morphology was observed by SEM and the results showed that the pollen morphology of *Bra-MIR319b* and *Bra-MIR319c* transgenic plants did not differ from that of wild-type plants (Figure 4g–h and k–l). However, these aborted pollen grains of *Bra-MIR319a* overexpressing plants were shrunk (Figure 4f,j). Thus, the results showed that *Bra-MIR319* family members had functional differentiation in pollen development, and the overexpression of *Bra-MIR319a* could lead to remarkable pollen abortion.

### 3.4. *Bra-MIR319a* Overexpressing in *Arabidopsis* Affects the Formation of Pollen Content and Intine

We observed anthers at different developmental stages via semithin section analysis to clarify the underlying reasons for pollen abortion in *Bra-MIR319a* overexpressing transgenic *Arabidopsis* plants. Until the early uninucleate stage, no difference was observed between *Bra-MIR319a* transgenic plants and wild-type plants (Figure 5a–b,e–f). The results of semithin sectioning revealed that at the binuclear stage, *Bra-MIR319a* transgenic plants showed vacuolar pollen, and the vacuolar pollen completely shrunk at the mature pollen stage (Figure 5g–h). TEM was used for more detailed observation. The results of TEM showed that the pollen content of *Bra-MIR319a* transgenic plants began to degrade from the uninucleate vacuole stage and continued to degrade in the binuclear stage, with complete

degradation during the mature pollen stage (Figure 6f–h). With the degradation of the pollen content, the pollen intine of the *Bra-MIR319a* transgenic plant disappeared with the intact structure of pollen exine (Figure 6i–j). These findings suggest the overexpression of *Bra-MIR319a* led to the degradation of pollen contents, thereby affecting the formation of pollen intine and leading to pollen distortion.

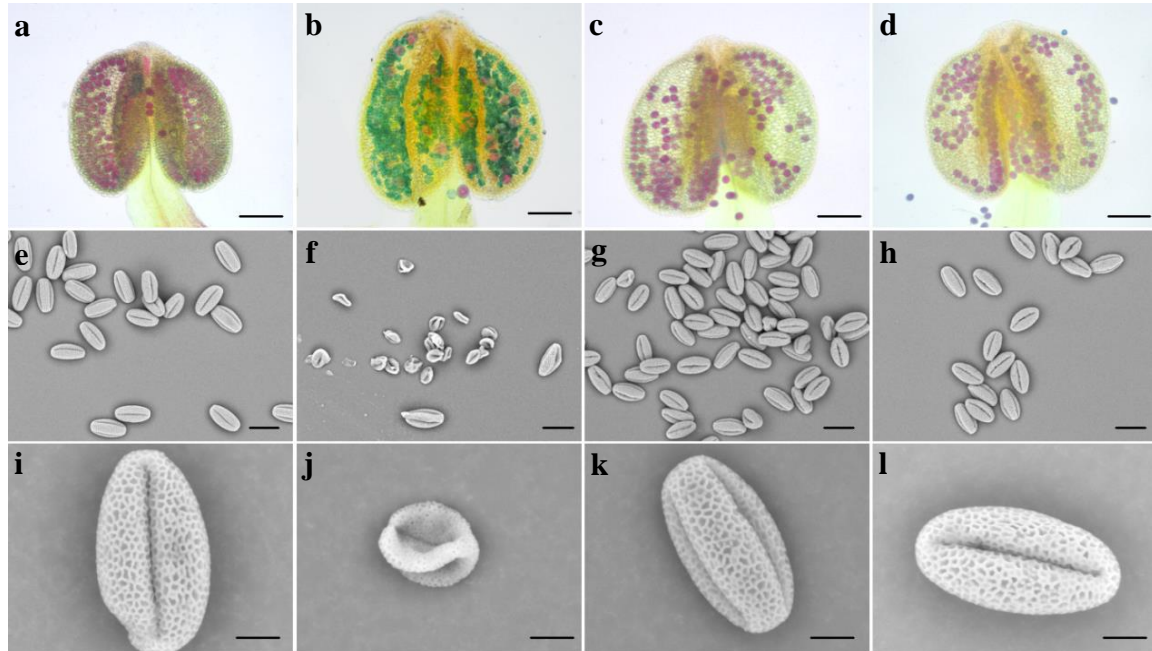


**Figure 4.** Morphological observation of pollen grains of *Bra-MIR319* family overexpressing transgenic *Arabidopsis*. (a–d) Alexander staining of anthers of wild-type and *Bra-MIR319* family transgenic *Arabidopsis*, respectively. (e,i) SEM observation of mature pollen grains of wild-type plants, (f,j) *Bra-MIR319a* transgenic plants, (g,k) *Bra-MIR319b* transgenic plants, and (h,l) *Bra-MIR319c* transgenic plants. Scale bars, 25  $\mu\text{m}$  in (a–h), 50  $\mu\text{m}$  in (i–l).

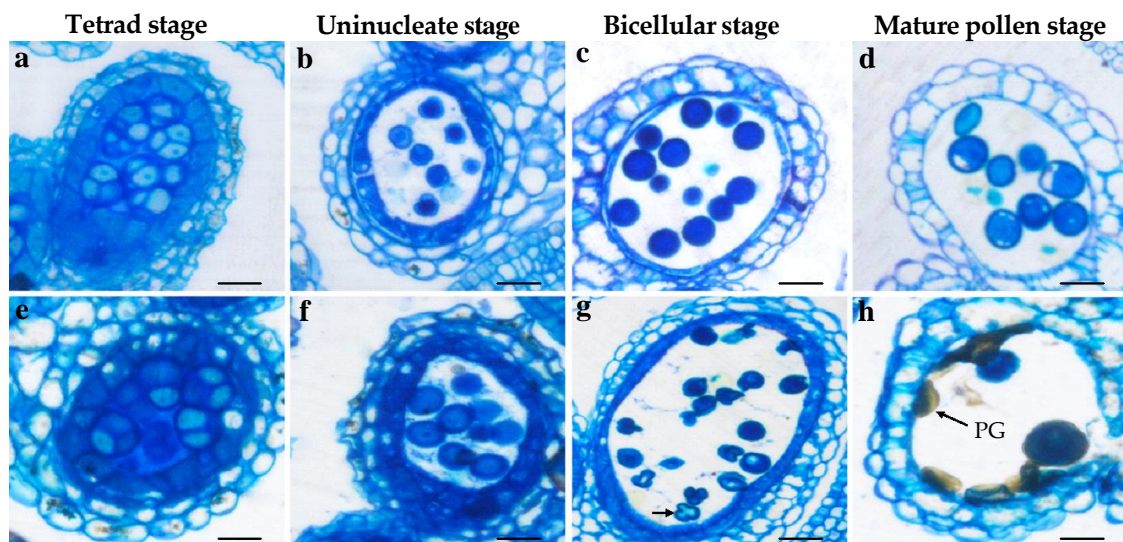


**Figure 5.** Semithin section observation of anther development in *Bra-MIR319a* overexpressing transgenic *Arabidopsis*. (a–d) Different anther development stages of wild-type plants and *Bra-MIR319a* transgenic plants (e–h). Arrows show the abnormal microspores. PG, pollen grain. Scale bars, 50  $\mu\text{m}$ .

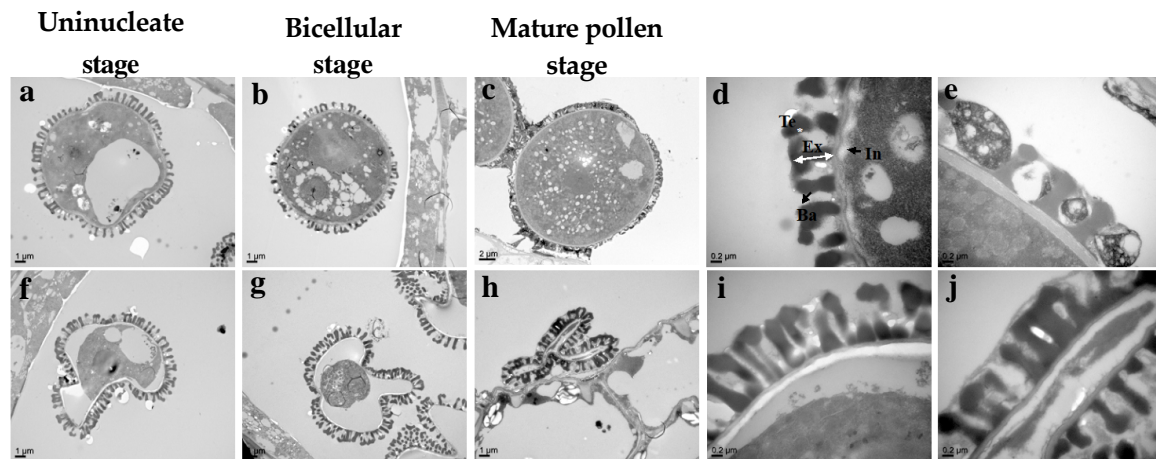


**Figure 6.** TEM observation of pollen grain in *Bra-MIR319a* overexpressing transgenic *Arabidopsis*. (a–c) Different development stages of wild-type plants and *Bra-MIR319a* transgenic plant pollen grains (f–h). (d,e) and (i,j), magnified images of (b,c) and (g,h). Te, tectum; Ba, baculum; Ex, exine; In, intine.

### 3.5. *Bra-miR319a* Can Target Homologs of *MYB101*

In *Arabidopsis*, since miR319a also targeted *MYB33* and *MYB65*, some overexpression of miR319a plants could lead to additional stamen defects resembling those of *35S:miR159a* plants. However, after WGT, homologs of *MYB33* were not detected in any of the *Brassica* species and the miRNA-binding region was entirely missing in homologs of *MYB65* in *B. campestris* [6,22]. According to the analysis results of the miRNA target gene prediction website, we found *Bra-miR319a* could target homologs of *MYB101*. In *B. campestris*, homologs of *MYB101* had three copies: *BcMYB101-1* (Bra022888), *BcMYB101-2* (Bra021791), and *BcMYB101-3* (Bra005597). The results of the 5' RACE experiment proved that *Bra-miR319a* could cleave *BcMYB101-1* between nucleotides 10 and 11 of the miRNA recognition sequence (Figure 7a). Moreover, we transiently expressed the *BcMYB101-1*: GFP fusion protein in *N. benthamiana* leaves and coexpressed it with *Bra-miR319a*. As expected, the coexpression of *Bra-miR319a* led to the disappearance of GFP fluorescence (Figure 7c). As a control, we prepared a version of *BcMYB101-1*: GFP with multiple mutations in the miRNA complementary motif (Figure 7b), and when coexpressed with *Bra-miR319a*, the GFP signal still existed (Figure 7c). These data indicated that the regulation of target genes by *Bra-miR319a* was differentiated after WGT.

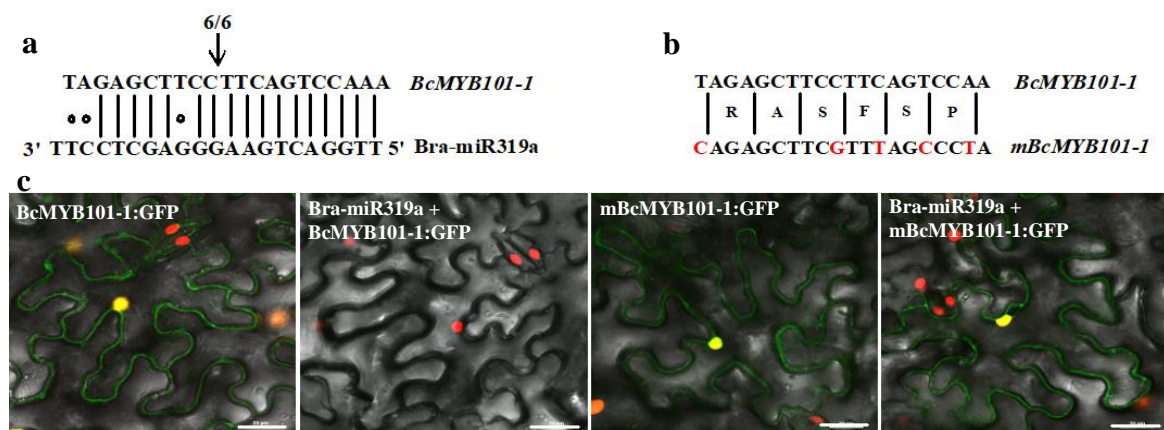


**Figure 7.** Specific regulation of *BcMYB101-1* by *Bra-miR319a*. (a) Validation of the target gene *BcMYB101-1* of *Bra-miR319a* in *B. campestris* by 5' RACE. (b) Construct of a version of *BcMYB101-1*: GFP with multiple mutations in the miRNA complementary motif. (c) Effects of *Bra-miR319a* on *BcMYB101-1*: GFP fluorescence in *Nicotiana benthamiana* leaf epidermal cells.

#### 4. Discussion

In Brassicaceae, *MIR319a* and *MIR319b* were closely related and formed sister clades, with *MIR319c* forming a separate clade [23]. In *Arabidopsis*, the expression of *MIR319a* was high during plant development. *MIR319a* overexpressing plants had crinkly leaves, whereas those with *MIR319c* overexpression had normal leaves due to limited expression during vegetative growth. Therefore, miR319a played a major role in leaf development [6,7]. In contrast to the expression pattern of *MIR319* members in *Arabidopsis*, *Bra-MIR319a* and *Bra-MIR319c* had similar expression patterns, whereas *Bra-MIR319b* was only expressed in the stem (Figure 1b). The overexpression of *Bra-MIR319c* could produce a leaf phenotype similar to that of plants overexpressing *Bra-MIR319a* (Figure 2a). The overexpression of *Brassica oleracea* *MIR319c* in *Arabidopsis* could also produce crinkled leaves, whereas the overexpression of *B. oleracea* *MIR319a* resulted in normal rosette leaves because the mature sequence of *Bol-MIR319a* differed in a single nucleotide from others. Thus, the function of the *MIR319a* gene in *B. oleracea* was assumed by *Bol-MIR319c* or *Bol-MIR319b* [24]. However, the mature sequence of *MIR319a* in *B. campestris* was the same as that of *A. thaliana* and could lead to similar crinkled leaves. Thus, *Bra-MIR319* family members had functional similarity in leaf development and could all give rise to functional Bra-miR319 in *A. thaliana*.

In *Arabidopsis*, miR319a could target some TCP transcription factors to inhibit cell division through different pathways [8,9]. In our study, SEM showed that the number of epidermal cells in *Bra-MIR319* family member transgenic plant leaves was reduced, and the shapes of epidermal cells were undifferentiated (Figure 3b–d). According to the miRNA target gene prediction website, Bra-miR319 family members could also target homologs of *TCP3* and *TCP4*, so we presumed that Bra-miR319 had similar regulatory pathways as those in *Arabidopsis* to affect cell division and differentiation. In addition, miR319-regulated *TCP4* could directly activate *YUCCA5* and integrate the auxin response to promote cell elongation in *A. thaliana* hypocotyls [25]. Overexpression of *Bra-MIR319* family members could also cause the size of the epidermal cells to increase, but it needed more experiments to illustrate the function of the *Bra-MIR319* family in the auxin pathway. Bra-miR319 family members had more functions in petal morphogenesis. Petals could be compared with the leaf lamina because both were broadly extended and positioned distally [26]. Thus, the overexpression of Bra-miR319 family members could also cause wavy petals and even cause the petals to darken (Figure 2i–l). In *Arabidopsis*, overexpression of *MIR319a* could affect the accumulation of chlorophyll and delay leaf senescence, and in double mutant *mir319ab*, the content of chlorophyll began to decline earlier than the wild-type plants [7,27]. So, we speculated the dark green color of the petals of *Bra-MIR319* overexpressing plants might be caused by chlorophyll accumulation.

*Bra-MIR319a* could be expressed in inflorescence and caused 86% pollen abortion. *Bra-MIR319a* overexpressing in *Arabidopsis* gave rise to the degradation of pollen contents from the uninucleate stage, and the pollen intine of transgenic plants disappeared (Figure 6f–j). Pollen contents provided the raw material for the formation of pollen intine [28]. During the uninucleate stage, pollen intine started forming and thickened in the binuclear stage. Thus, the pollen grain remained normal in form; however, abnormal development of pollen intine caused the pollen grain to shrink and led to abortion [29]. In *Arabidopsis*, except *TCPs*, miR319 could also target *MYB33* and *MYB65* and caused anther defects similar to miR159 [6]. However, after WGT in *B. campestris*, homologs of *MYB33* were lost [6,21]. In this study, we confirmed that Bra-miR319a could target homologs of *MYB101* (Figure 7). *MYB101*, *MYB120*, and *MYB97* had functional redundancy in pollen tube growth in *Arabidopsis* [30]. In *B. campestris*, homologs of *MYB97* were lost, and *BcMYB101* and *BcMYB120* each had three copies, whereas Bra-miR319a could only target one copy of *BcMYB101*. Thus, we inferred that they might exhibit functional differentiation. Bra-miR319a might function in pollen development by regulating *BcMYB101-1*. In our future work, we will investigate the relevant detailed mechanisms. Although *Bra-MIR319c* had similar expression in the inflorescence, it did not cause pollen abortion when overexpressed in *Arabidopsis*. However, when *Bra-MIR319c* was overexpressed in *B. campestris*

ssp. *chinensis* cv. Youqin 49, it could cause 25% pollen abortion [17]. We suspect that Bra-miR319c played a minor role in pollen development.

In conclusion, *Bra-MIR319* family members had different expression patterns, but they had functional similarity in leaf and petal morphogenesis. Moreover, we revealed that the overexpression of *Bra-MIR319a* in *Arabidopsis* played a role in pollen intine formation and caused pollen grains to shrink. This study helps us to deepen our understanding of the similarity and difference of miRNA function in the same family and to explore new miRNA regulatory networks formed after replication events.

**Supplementary Materials:** The following are available online at <http://www.mdpi.com/2073-4425/10/12/952/s1>, Figure S1: Expression analysis of *Bra-MIR319a*; Table S1: Primers used in this article.

**Author Contributions:** Z.H. designed all the experiments. T.L. took part in this work and the manuscript modification. J.C. is the corresponding author. All authors read and approved the final manuscript.

**Funding:** This work was supported by the National Natural Science Foundation of China (No. 31772311).

**Conflicts of Interest:** All authors declare that they have no conflict of interest.

## References

1. Jones-Rhoades, M.; Bartel, D.; Bartel, B. MicroRNAs and Their Regulatory Roles in Plants. *Annu. Rev. Plant Biol.* **2006**, *57*, 19–53. [[CrossRef](#)] [[PubMed](#)]
2. Li, A.; Mao, L. Evolution of plant microRNA gene families. *Cell Res.* **2007**, *17*, 212–218. [[CrossRef](#)] [[PubMed](#)]
3. Zou, Q.; Mao, Y.; Hu, L.; Wu, Y.; Ji, Z. miRClassify: An advanced web server for miRNA family classification and annotation. *Comput. Biol. Med.* **2014**, *45*, 157–160. [[CrossRef](#)]
4. Barik, S.; SarkarDas, S.; Singh, A.; Gautam, V.; Kumar, P.; Majee, M.; Sarkar, A.K. Phylogenetic analysis reveals conservation and diversification of microRNA166 genes among diverse plant species. *Genomics* **2014**, *103*, 114–121. [[CrossRef](#)] [[PubMed](#)]
5. Palatnik, J.F.; Allen, E.; Wu, X.; Schommer, C.; Schwab, R.; Carrington, J.; Weigel, D. Control of leaf morphogenesis by microRNAs. *Nature* **2003**, *425*, 257–263. [[CrossRef](#)] [[PubMed](#)]
6. Palatnik, J.F.; Wollmann, H.; Schommer, C.; Schwab, R.; Boisbouvier, J.; Rodriguez, R.; Warthmann, N.; Allen, E.; Dezulian, T.; Huson, D.; et al. Sequence and expression differences underlie functional specialization of *arabidopsis* microRNAs miR159 and miR319. *Dev. Cell* **2007**, *13*, 115–125. [[CrossRef](#)] [[PubMed](#)]
7. Koyama, T.; Sato, F.; Ohme-Takagi, M. Roles of miR319 and TCP transcription factors in leaf development. *Plant Physiol.* **2017**, *175*, 874–885. [[CrossRef](#)]
8. Bresso, E.G.; Chorostecki, U.; Rodriguez, R.E.; Palatnik, J.F.; Schommer, C. Spatial control of gene expression by miR319-regulated TCP transcription factors in leaf development. *Plant Physiol.* **2018**, *176*, 1694–1708. [[CrossRef](#)]
9. Schommer, C.; Debernardi, J.M.; Bresso, E.G.; Rodriguez, R.E.; Palatnik, J.F. Repression of cell proliferation by miR319-regulated *TCP4*. *Mol. Plant* **2014**, *7*, 1533–1544. [[CrossRef](#)] [[PubMed](#)]
10. Grant-Downton, R.; Le Trionnaire, G.; Schmid, R.; Rodriguez-Enriquez, J.; Hafidh, S.; Mehdi, S.; Twell, D.; Dickinson, H. MicroRNA and tasiRNA diversity in mature pollen of *Arabidopsis thaliana*. *BMC Genom.* **2009**, *10*, 643. [[CrossRef](#)] [[PubMed](#)]
11. Ryder, C.D.; Smith, L.B.; Teakle, G.R.; King, G.J. Contrasting genome organisation: Two regions of the *Brassica oleracea* genome compared with collinear regions of the *Arabidopsis thaliana* genome. *Genome* **2001**, *44*, 808–817. [[CrossRef](#)]
12. Wang, X.; Wang, H.; Wang, J.; Sun, R.; Wu, J.; Liu, S.; Bai, Y.; Mun, J.H.; Bancroft, I.; Cheng, F. The genome of the mesopolyploid crop species *Brassica rapa*. *Nat. Genet.* **2011**, *43*, 1035–1039. [[CrossRef](#)] [[PubMed](#)]
13. Sun, C.; Wu, J.; Liang, J.; Schnable, J.C.; Yang, W.; Cheng, F.; Wang, X. Impacts of whole-genome triplication on *MIRNA* evolution in *Brassica rapa*. *Genome Biol. Evol.* **2015**, *7*, 3085–3096. [[CrossRef](#)] [[PubMed](#)]
14. Jain, A.; Das, S. Synteny and comparative analysis of miRNA retention, conservation, and structure across Brassicaceae reveals lineage-and sub-genome-specific changes. *Funct. Integr. Genom.* **2016**, *16*, 253–268. [[CrossRef](#)]
15. Xie, J.; Yang, X.; Song, Y.; Du, Q.; Li, Y.; Chen, J.; Zhang, D. Adaptive evolution and functional innovation of *Populus*-specific recently evolved microRNAs. *New Phytol.* **2017**, *213*, 206–219. [[CrossRef](#)]

16. Chávez Montes, R.A.; De Fátima Rosas-Cárdenas, F.; De Paoli, E.; Accerbi, M.; Rymarquis, L.A.; Mahalingam, G.; Marsch-Martínez, N.; Meyers, B.C.; Green, P.J.; De Folter, S. Sample sequencing of vascular plants demonstrates widespread conservation and divergence of microRNAs. *Nat. Commun.* **2014**, *5*, 3722. [[CrossRef](#)] [[PubMed](#)]
17. Hu, Z.W.; Shen, X.P.; Xiang, X.; Cao, J. Evolution of *MIR159/319* genes in *Brassica campestris* and their function in pollen development. *Plant Mol. Biol.* **2019**. [[CrossRef](#)]
18. Livak, K.; Schmittgen, T. Analysis of relative gene expression data using real-time quantitative PCR and the  $2^{-\Delta\Delta CT}$  method. *Methods* **2001**, *25*, 402–408. [[CrossRef](#)] [[PubMed](#)]
19. Zhang, X.; Henriques, R.; Lin, S.S.; Niu, Q.W.; Chua, N.H. *Agrobacterium*-mediated transformation of *Arabidopsis thaliana* using the floral dip method. *Nat. Protoc.* **2006**, *1*, 641–646. [[CrossRef](#)] [[PubMed](#)]
20. Lin, S.; Dong, H.; Zhang, F.; Qiu, L.; Wang, F.; Cao, J.; Huang, L. *BcMF8*, a putative arabinogalactan protein-encoding gene, contributes to pollen wall development, aperture formation and pollen tube growth in *Brassica campestris*. *Annu. Bot.* **2014**, *10*, 1093. [[CrossRef](#)]
21. Shen, X.; Xu, L.; Liu, Y.; Dong, H.; Zhou, D.; Zhang, Y.; Lin, S.; Cao, J.; Huang, L. Comparative transcriptome analysis and ChIP-sequencing reveals stagespecific gene expression and regulation profiles associated with pollen wall formation in *Brassica rapa*. *BMC Genom.* **2019**, *20*, 264–287. [[CrossRef](#)]
22. Anand, S.; Lal, M.; Das, S. Comparative genomics reveals origin of *MIR159A-MIR159B* paralogy, and complexities of PTGS interaction between miR159 and target *GA-MYBs* in Brassicaceae. *Mol. Genet. Genom.* **2019**, *294*, 693–714. [[CrossRef](#)]
23. Joshi, G.; Chauhan, C.; Das, S. Microsynteny analysis to understand evolution and impact of polyploidization on *MIR319* family within Brassicaceae. *Dev. Genes. Evol.* **2018**, *228*, 227–242. [[CrossRef](#)] [[PubMed](#)]
24. Warthmann, N.; Das, S.; Lanz, C.; Weigel, D. Comparative analysis of the *MIR319a* microRNA locus in *Arabidopsis* and related Brassicaceae. *Mol. Biol. Evol.* **2008**, *25*, 892–902. [[CrossRef](#)] [[PubMed](#)]
25. Challa, K.R.; Aggarwal, P.; Nath, U. Activation of *YUCCA5* by the Transcription Factor TCP4 Integrates Developmental and Environmental Signals to Promote Hypocotyl Elongation in *Arabidopsis*. *Plant Cell.* **2016**, *28*, 2117–2130. [[CrossRef](#)]
26. Crawford, B.C.; Nath, U.; Carpenter, R.; Coen, E.S. *CINCINNATA* controls both cell differentiation and growth in petal lobes and leaves of *Antirrhinum*. *Plant Physiol.* **2004**, *135*, 244–253. [[CrossRef](#)] [[PubMed](#)]
27. Schommer, C.; Palatnik, J.F.; Aggarwal, P.; Chételat, A.; Cubas, P.; Farmer, E.E.; Nath, U.; Weigel, D. Control of jasmonate biosynthesis and senescence by miR319 targets. *PLoS Biol.* **2008**, *6*, e230. [[CrossRef](#)]
28. Yeung, E.C.; Oinam, G.S.; Yeung, S.S.; Harry, I. Anther, pollen and tapetum development in safflower, *Carthamus tinctorius* L. *Sex. Plant Reprod.* **2011**, *24*, 307–317. [[CrossRef](#)] [[PubMed](#)]
29. Drakakaki, G.; Zabolina, O.; Delgado, I.; Robert, S.; Keegstra, K.; Raikhel, N. *Arabidopsis* reversibly glycosylated polypeptides 1 and 2 are essential for pollen development. *Plant Physiol.* **2006**, *142*, 1480–1492. [[CrossRef](#)] [[PubMed](#)]
30. Liang, Y.; Tan, Z.M.; Zhu, L.; Niu, Q.K.; Zhou, J.J.; Li, M.; Chen, L.Q.; Zhang, X.Q.; Ye, D. *MYB97*, *MYB101* and *MYB120* function as male factors that control pollen tube-synergid interaction in *Arabidopsis thaliana* fertilization. *PLoS Genet.* **2013**, *9*, e1003933. [[CrossRef](#)]

